



HAL
open science

Moisture diffusion in plasma-enhanced chemical vapor deposition dielectrics characterized with three techniques under clean room conditions

Vivien Cartailier, Grégory Imbert, Névine Rochat, Catherine Chaton, Du Vo-Thanh, Daniel Benoit, Geneviève Duchamp, Hélène Frémont

► To cite this version:

Vivien Cartailier, Grégory Imbert, Névine Rochat, Catherine Chaton, Du Vo-Thanh, et al.. Moisture diffusion in plasma-enhanced chemical vapor deposition dielectrics characterized with three techniques under clean room conditions. *Thin Solid Films*, 2020, 698, pp.137874 -. 10.1016/j.tsf.2020.137874 . hal-03489597

HAL Id: hal-03489597

<https://hal.science/hal-03489597>

Submitted on 7 Mar 2022

HAL is a multi-disciplinary open access archive for the deposit and dissemination of scientific research documents, whether they are published or not. The documents may come from teaching and research institutions in France or abroad, or from public or private research centers.

L'archive ouverte pluridisciplinaire **HAL**, est destinée au dépôt et à la diffusion de documents scientifiques de niveau recherche, publiés ou non, émanant des établissements d'enseignement et de recherche français ou étrangers, des laboratoires publics ou privés.



Distributed under a Creative Commons Attribution - NonCommercial 4.0 International License

Title: Moisture diffusion in plasma-enhanced chemical vapor deposition dielectrics characterized with three techniques under clean room conditions

Authors: Vivien Cartailier^{a,b}, Grégory Imbert^b, Névine Rochat^c, Catherine Chaton^d, Du Vo-Thanh^b, Daniel Benoit^b, Geneviève Duchamp^a, Hélène Frémont^a

^a Laboratoire IMS, Université de Bordeaux, Talence, France

^b STMicroelectronics, Crolles, France

^c Univ. Grenoble Alpes, CEA, LETI, 38000 Grenoble, France

^d LETI-CEA Tech, 38000 Grenoble, France

Corresponding author:

Vivien Cartailier

E-mail address: vivien.cartailier@st.com

STMicroelectronics, 850 Rue Jean Monnet, Crolles, France

Phone : +33 04 38 92 31 65

Summary declaration of interest: Declarations of interest: none

Keywords: Moisture diffusion, Thin dielectric film, Silicon oxide, Plasma-enhanced chemical vapor deposition

Abstract

Absorption of moisture by thin dielectric materials alters their properties and can cause several reliability issues. Even at standard room temperature and low humidity level, some dielectric materials are sensitive to moisture. In this study, moisture diffusion in two plasma-enhanced chemical vapor deposition (PECVD) films is investigated with three measurement methods to determine diffusion coefficients and saturated moisture concentrations: mass measurements, bending radius of curvature measurements and infrared spectroscopy. The two PECVD silicon dioxides are deposited at 200°C and 400°C. They were exposed to moisture in clean room environment (21°C and 40% relative humidity) for about 800 hours. The present results confirm that mass measurements, bending radius of curvature measurements and infrared spectroscopy can be used to monitor thin dielectric films in these environmental conditions. They lead to similar values for the diffusion coefficient. These values are in the range of $[1.5-4.2] \times 10^{-15} \text{ cm}^2.\text{s}^{-1}$ for the 200°C film and $[2.3-3.6] \times 10^{-15} \text{ cm}^2.\text{s}^{-1}$ for the 400°C one. Saturated moisture concentrations confirm that the two dielectrics are sensitive to moisture even at 21°C, 40% relative humidity. Besides, the results show that standard fickean behavior does not provide the best fit to model water diffusion for some dielectric films. A dual stage model that appears to be more adapted is finally introduced.

1. Introduction

Moisture is responsible for a wide range of reliability problems in microelectronics. Although semiconductor chips are encapsulated, moisture permeates along interfaces or diffuses through the packaging materials. Only a small amount of water can strongly alter dielectric materials' properties. Moisture can weaken an interface between two layers and lead to delamination [1]. It can also cause electrochemical corrosion of metals [2]. Our observations show that moisture uptake already occurs at clean room conditions that are used during dielectric die production (21°C and 40% relative humidity (RH)). Hence, to improve reliability, a better understanding of water interaction with dielectrics is required.

Two parameters characterize water diffusion at a given temperature and humidity level: the diffusion coefficient D and the moisture-saturated concentration C_{sat} . When moisture diffuses into a layer, some of its electrical, chemical and mechanical properties are impacted. It is possible to obtain intrinsic diffusion parameters by monitoring these properties and fitting experimental data with an appropriate diffusion model.

From an experimental point of view, procedures have been designed to evaluate moisture diffusion into barrier layers. They depend on the type of substrate used for deposition. It can be polymer or silicon substrates depending on the application. In the organic light-emitting diode industry, polymer substrates are widely used. Moisture permeates through these substrates, which is adapted for specific permeation tests [3, 4]. The calcium test is also of interest but requires an additional deposition step [5, 6]. Moreover, these methods lead to the water vapor transmission rate and not directly to intrinsic material properties (such as diffusion coefficient). The intrinsic properties are necessary to compare with existing literature [7-9]; they can also be used for numerical simulations. Other techniques are of interest to determine intrinsic diffusion properties directly. Infrared spectroscopy was used over a wide range of temperatures to determine diffusion coefficients for silica glasses [10,

11]. It also gives valuable information on chemical bonds and their evolution. Bending radius of curvature measurements are also relevant to determine diffusion coefficients [12]. Mass measurements were used to find diffusion coefficients of polymers used for chip packaging under high temperatures and humidity levels [13]. But these techniques were proposed and used independently. For the comparison between experimental procedures, Visweswaran used three methods to obtain diffusion coefficient of a plasma-enhanced chemical vapor deposition (PECVD) barrier layer: secondary ion mass spectroscopy (SIMS), stress measurements and capacitance measurements [14]. In order to complete existing results, we propose a comparison of three measurement techniques – mass, bending radius of curvature (linked to stress with Stoney equation) and infrared spectroscopy – to determine diffusion parameters.

The present study has two goals. The first one is to compare the three measurement techniques mentioned above to confirm that they lead to same diffusion coefficient under Fickian behavior assumption. The second one is to show that moisture uptake is not negligible at ambient clean room conditions and diffusion properties can be studied in these conditions (21°C, 40% RH). We selected two production materials widely used: two PECVD silicon dioxide deposited at 200°C and 400°C.

The paper begins with the description of the two materials studied with their deposition parameters. The description of experimental techniques follows: mass, bending radius of curvature and infrared spectroscopy measurements. Then, the necessary equations to obtain diffusion coefficients are introduced. The subsequent sections present experimental results, limitations and discuss them.

2. Experimental details

2.1 Materials

Moisture diffusion has been studied for two materials: hydrogenated silicon dioxide (SiO₂:H) and hydrogenated N-doped silicon dioxide (N-doped SiO₂:H). Layers are deposited by PECVD (Producer from Applied Materials) on silicon substrates at 200°C (pressure of 467 Pa) for N-doped SiO₂:H and 400°C for SiO₂:H (pressure of 320 Pa). The plasma frequency is 13.56 MHz for both films. RF power is 2 150 W for SiO₂:H and 340 W for N-doped SiO₂:H. Precursors are nitrous oxide (N₂O) and silane (SiH₄ with a ratio SiH₄/N₂O of 0.05) for SiO₂:H. For N-doped SiO₂:H, ammonia (NH₃ with a ratio NH₃/N₂O of 0.23), N₂O and SiH₄ (with a ratio SiH₄/N₂O of 0.04) are used. The deposition rate is 14 nm/s for SiO₂:H and 3.5 nm/s for the N-doped layer.

The silicon wafer substrates were 300 mm diameter, 780 μm thick, double-side polished for IR spectroscopy, P-type and <100> oriented. The oxidized surface on substrate was characterized with ellipsometry. The thickness measured is 1.3 nm ± 0.1 (mean value over 17 measurements). The mass and bending radius of curvature of a substrate were monitored in clean room conditions for several months. No variation is observed over time.

Table 1 shows thickness-and intrinsic stress right after deposition. Thickness is controlled with deposition duration. The intrinsic stress calculation is explained in 2.2.2. Negative values represent compressive stress and positive values represent tensile stress.

2.2 Methods

One wafer for each material was used. They were stored in clean room environment at 21°C and 40% relative humidity. Characterization tools are all located in the same clean room to perform measurements in the same environmental conditions. The three techniques were applied first on the substrate alone (before deposition), then immediately after deposition to deduct as deposited properties for each material (Table 1). Wafers were monitored over 800 hours.

2.2.1 Infrared spectroscopy

Fourier transform infrared spectrometer (QS3300 from Nanometrics) was used to obtain transmission spectra in the range of 400 to 4000 cm^{-1} with a resolution of 6 cm^{-1} . The analysis has been carried out in normal incidence transmission mode. Each spectrum was converted in absorbance baseline, then baseline corrected and finally was normalized with respect to the layer thickness.

2.2.2 Mass

Commercial tool from METRYX was used to perform mass monitoring. Measurement uncertainty is 40 μg . Since materials are stored in a clean room, there is no contamination source. Hence, we assume that the mass uptake is only due to moisture diffusion and is homogeneous over the entire thickness. M_0 corresponds to the mass after deposition and M_∞ to the mass measured after saturation. With the previous assumption, the saturated mass uptake ΔM is given by:

$$\Delta M = M_\infty - M_0 \quad (1)$$

Saturated moisture concentration C_{sat} is obtained from the saturated mass uptake and layer volume V as follow:

$$C_{\text{sat}} = \frac{\Delta M}{V} \quad (2)$$

2.2.3 Stress

Bending radius of curvature monitoring was performed on a Frontier Semiconductor Measurements tool (128L C2C). Measurement principle has been described elsewhere [12]. Bending radius of curvature is related to stress with Eq. (3). We measured warpage of the silicon substrate alone to consider it in Eq. (3). When dielectric films absorb water, they swell.

Because of the silicon substrate, the swelling is constrained and the wafer bends. Stress $\sigma(t)$ and bending radius of curvature $R(t)$ are related with the Stoney equation [15]:

$$\sigma(t) = \frac{E_S}{6(1-\nu_S)} \frac{h_S^2}{h} \left(\frac{1}{R(t)} - \frac{1}{R_0} \right) \quad (3)$$

R_0 is the bending radius of curvature before deposition, E_S , ν_S and h_S are the Young's modulus, the Poisson's ratio and the thickness of the silicon wafer.

The PECVD thin films studied are deposited on thick silicon substrate. We confirmed that the deformation is spherical by measuring wafers along several diameters. Hence, hypotheses required for the Stoney formula are respected [16].

2.3 Data extraction

Materials are deposited on a silicon substrate. They eventually saturate with water through their entire thickness h . Crank described the number of water molecules that has entered the layer the material at time t . It is given by Eq. (4.18) in [17]:

$$\frac{N(t)}{N_\infty} = 1 - \sum_{k=0}^{\infty} \frac{8}{(2k+1)^2 \pi^2} e^{-\frac{D(2k+1)^2 \pi^2 t}{4h^2}} \quad (4)$$

Where $N(t)$ is the number of water molecules per unit surface area absorbed at t , N_∞ is the corresponding quantity after infinite time, D is the diffusion coefficient.

This equation can be applied to any material properties changing as a function of the parameter $N(t)$. Hence, we monitored mass uptake, stress variations and infrared spectroscopy results and fitted them with Eq. (5).

$$\frac{X(t)}{X_\infty} = 1 - \sum_{k=0}^{\infty} \frac{8}{(2k+1)^2 \pi^2} e^{-\frac{D(2k+1)^2 \pi^2 t}{4h^2}} \quad (5)$$

X can stand for mass uptake, stress variations or water related peaks variations.

We use the method of least squares, under Scilab©, to find the diffusion coefficient value which minimizes S in Eq. (6).

$$S = \sum_i \left(X_{exp}(t_i) - X_{th}(t_i) \right)^2 \quad (6)$$

Where X_{exp} and X_{th} are, respectively, the experimental and theoretical values obtained with Eq. (5).

3. Results

Fig. 1 (a) shows the IR absorption spectra of SiO₂:H and N-doped SiO₂:H immediately after deposition. Both materials have similar structure. They present the characteristic Si-O-Si absorption peaks: stretching mode at 1080 cm⁻¹ ($\nu_{Si-O-Si}$), wagging mode at 800 cm⁻¹ ($\delta_{Si-O-Si}$) and rocking mode at 450 cm⁻¹ ($\beta_{Si-O-Si}$) [18]. Both materials exhibit N-H stretching mode at ~3375 cm⁻¹ (ν_{N-H}) due to their precursors. Nitrogen concentration is low in both materials, we assume it does not affect variations in the 2800-3800 cm⁻¹ range (i.e. ν_{N-H} at 3375 cm⁻¹ is constant over storage time).

After moisture saturation, the spectra of both materials evolve as shown in Fig. 1 (b), which presents IR absorption spectra over 2800 cm⁻¹ to 3800 cm⁻¹. This range corresponds to water related bonds.

For the SiO₂:H, the area homogeneously increases over the whole range. For the N-doped SiO₂:H, the increase concerns the area from 3000 cm⁻¹ to 3300 cm⁻¹. This range corresponds to free molecular water. There is also a difference between the two layers around 3600 cm⁻¹ that can be interpreted as a variation of Si-OH. As our objective is to test a simple and straightforward method to determine the diffusion coefficient, we did not focus on these phenomenon and further investigations are required. Hence, the area under IR curves is integrated between 2800 cm⁻¹ and 3800 cm⁻¹ to integrate all type of OH species from water molecules to dissociated OH, after layer depositions and after time intervals. Area values are then injected in Eq. (5).

Fig. 2 and 3 illustrate mass uptake (a), stress variations (b) and water related infrared area variations (c) as a function of the square root of time for SiO₂:H and N-doped SiO₂:H. The experimental data are fitted with Eq. (5) presented in 2.3 as a first approach. The agreement between the data and the model is correct except a deviation observed at short times for both materials. This will be discussed in the latter part. Nevertheless, the agreement is sufficient to extract diffusion coefficients, saturated moisture concentration. Results are given in Table 2 for both layers. Three values of diffusion coefficient are given, for each material, depending on the measurement methods. Saturated moisture concentrations obtained with mass monitoring are also presented.

All three techniques yield to comparable values in the range $[2.3-3.6].10^{-15} \text{ cm}^2.\text{s}^{-1}$ for SiO₂:H and $[1.5-4.2].10^{-15} \text{ cm}^2.\text{s}^{-1}$ for N-doped SiO₂:H. The saturated moisture concentrations are calculated from saturated mass uptake in Fig. 2 (a) and Fig. 3 (a), which are injected in Eq. (2). Higher mass uptake for the N-doped layer is consistent with the higher variations observed with infrared spectroscopy and stress.

4. Discussion

4.1 Diffusion coefficients and saturated moisture concentrations

For both materials, values calculated with infrared spectroscopy are slightly higher than those deduced from the two other methods. Fewer measurements were done with this technique and more steps are required to process the data compared to the other methods (baseline correction, integration limits choice). Moreover, we observe more disparity for the N-doped layer. The differences previously discussed in the previous part (3. Results) concerning IR spectra of both materials could explain the higher disparity observed for the N-doped layer.

Table 3 summarizes diffusion coefficients for similar materials found in literature. Although materials in the table are similar, they differ in their deposition parameters. It can explain the

variation observed over the diffusion coefficient values. Nonetheless, the values found in this paper are consistent with literature.

Concerning saturated moisture concentration, few values at ambient are available in the literature concerning dielectric materials. Viswevaran found a normalized solubility between 2×10^{-2} and $3 \times 10^{-2} \text{ g.cm}^{-3}.\text{atm}^{-1}$ for SiO₂-silicone hybrid at ambient temperature and 100% RH (with an extrapolation from experiments at higher temperatures). It corresponds to a saturated moisture concentration between $6 \times 10^{-1} \text{ mg.cm}^{-3}$ and $9 \times 10^{-1} \text{ mg.cm}^{-3}$. More values are available for polymers. He and Fan measured a saturated moisture concentration around 4 mg.cm^{-3} at 30°C for a 70 μm bismaleimide-triazine (BT)/glass fiber laminated substrate core material [21]. Moylan found values in the range of $18 \pm 7 \text{ mg.cm}^{-3}$ to $111 \pm 12 \text{ mg.cm}^{-3}$ for four different polyimides at 22°C [22]. These values are either found for thick samples (>10μm) or with different techniques like SIMS [14]. However, our results [17 and 41 mg.cm^{-3}] are in the same range.

4.2 Method consideration

We investigated three methods to determine diffusion parameters at ambient conditions. A good agreement is found between them. Among them, the mass measurement method is the only one that provides both diffusion coefficient and saturated moisture concentration, which are key material properties to assess water diffusion. If water diffusion is monitored only regarding stress, it will lead to the diffusion coefficient and a stress variation. A calibration with a known mass uptake is necessary to get the saturated moisture concentration.

In order to evaluate the limitation of the three methods, we monitored other common dielectric materials in the same conditions (SiO₂ and SiN type). All minimal variations observable are converted into mass gain to compare the three techniques. Table 4 summarizes the results. Infrared spectroscopy is the less sensitive one and requires a higher water uptake

to calculate diffusion coefficient. It could explain, in addition to the reasons already mentioned, the difference observed for diffusion coefficients of SiO₂:H and N-doped SiO₂:H.

Another limitation could be due to some simplifying assumptions. Water diffusion and sorption were assumed homogeneous in the layers studied. But, the three techniques do not inform on the local specificities of water diffusion and surface phenomena are not analyzed. To support the homogeneity assumption, it is possible to calculate the mass of one monolayer of water on the wafer. The diameter for a molecule of water is 0.34 nm. Considering a spherical assumption to simplify calculus and knowing molecular mass of water and wafer dimensions (diameter of 300 mm), it leads to a mass of approximately 23 µg for a monolayer over the entire wafer. We found saturated mass of 720 µg (SiO₂) and 1600 µg (N-doped SiO₂). A few water layers on the top surface do not explain the important mass uptake measured and most of the sorption occurs in the bulk. Hence, the homogeneity assumption is still reasonable.

4.3 Model Improvement

The results confirmed that the three techniques lead to similar water diffusion coefficient assuming Fickian diffusion. However, from Fig. 2 and 3, it can be seen that experimental data in the first hours are not correctly fitted. This is probably due to a non-perfect Fickian behavior of this type of materials.

Fig. 4 presents the mass uptake and the stress variations as a function of square root of time. To fit the experimental data we used two models: the one previously described in 2.3. and a dual stage model [23]. This model was successfully applied to describe absorption and desorption processes during aging (85°C/85% RH) of epoxy mold compounds. It assumes two ongoing diffusion mechanisms as described with Eq. (7):

$$N(t) = N_{1,\infty} \left[1 - \sum_{k=0}^{\infty} \frac{8}{(2k+1)^2 * \pi^2} e^{-\frac{D_1(2k+1)^2 \pi^2 t}{4h^2}} \right] + N_{2,\infty} \left[1 - \sum_{k=0}^{\infty} \frac{8}{(2k+1)^2 * \pi^2} e^{-\frac{D_2(2k+1)^2 \pi^2 t}{4h^2}} \right] \quad (7)$$

With: $N_{\infty} = N_{1,\infty} + N_{2,\infty}$ (8) where N_{∞} is the total number of water molecule after infinite time. Under assumption that both these mechanisms affect mass and stress variations, we propose the following equation:

$$X(t) = X_{1,\infty} \left[1 - \sum_{k=0}^{\infty} \frac{8}{(2k+1)^2 * \pi^2} e^{-\frac{D_1(2k+1)^2 \pi^2 t}{4h^2}} \right] + X_{2,\infty} \left[1 - \sum_{k=0}^{\infty} \frac{8}{(2k+1)^2 * \pi^2} e^{-\frac{D_2(2k+1)^2 \pi^2 t}{4h^2}} \right] \quad (9)$$

Where X can stand for mass uptake or stress variations and $X_{\infty} = X_{1,\infty} + X_{2,\infty}$ (10) where X_{∞} can stand for the total mass uptake or total stress variation.

Fig. 4 shows experimental data fitted with the dual stage model from Eq. (9). For SiO_2 , (a) and (c) are respectively for mass monitoring and stress monitoring. For N-doped SiO_2 , (b) represents the fitting for mass monitoring and (d) for stress monitoring. It gives a better fitting compared to the classic Fick model. This is confirmed with Table 5 that gives values for parameter S from Eq. (6). For each case an improvement is obtained when the dual stage model is used compared to the Fick model.

Parameters for each model are given in Table 6. Optimizations for the dual stage model were also done under Scilab. Each diffusion mechanism is characterized with a couple of parameters ($D_i, X_{i,\infty}$).

For instance, we obtain ($5.7 \times 10^{-13} \text{ cm}^2 \cdot \text{s}^{-1}$, $185 \mu\text{g}$) for one mechanism with mass monitoring for SiO_2 . The saturated value $185 \mu\text{g}$ corresponds to the end of the first linear part of the curve, as it can be seen on Fig. 4 (a). The total mass uptake is $725 \mu\text{g}$. Hence, this mechanism represents 26% of the total uptake. Same reasoning can be applied with stress values.

A good agreement is found again between stress and mass monitoring. They yield similar values for diffusion coefficients and saturated values. It confirms the excellent agreement between these two techniques even under a different model.

Besides, the dual stage model seems to be adapted to describe water diffusion in some dielectric materials. We assume that moisture diffusion takes place in two phases. A fast diffusion into the free volume of materials (nano pores). Here, it corresponds to the first term in Eq.7 and is characterized by $(D_1, X_{1,\infty})$. The second term of Eq.7 characterized by $(D_2, X_{2,\infty})$ corresponds to the bonding of moisture with materials bulk, which is slower than the first mechanism. Further work is needed to confirm this assumption.

Hence, unlike it is usually assumed, some dielectrics are not Fickian. Diffusion behavior should be assessed first to select the proper model and avoid mistakes concerning diffusion parameters.

4. Conclusion

We monitored a 600 nm SiO₂ and a 550 nm N-doped SiO₂ at ambient conditions (21°C, 40% RH). An excellent agreement has been found between three techniques to determine diffusion coefficient: mass, bending radius of curvature and infrared spectroscopy measurements. For SiO₂ deposited at 400°C and N-doped SiO₂ deposited at 200°C, diffusion coefficients are in the range of, respectively, 2.3×10^{-15} to 3.6×10^{-15} cm².s⁻¹ and 1.5×10^{-15} to 4.2×10^{-15} cm².s⁻¹. Saturated moisture concentrations show that moisture uptake is significant for both materials at ambient.

The three methods are straightforward to obtain diffusion parameters. However, we found different behaviors between the two layers with infrared spectroscopy in the 3000 cm⁻¹ to 3800 cm⁻¹ area. It could explain the higher values for diffusion coefficients found with infrared spectroscopy.

Besides, Fick model does not fit experimental data with a good agreement in the first hours of diffusion for both layers. It suggests a non Fickian behavior for some dielectric materials. To illustrate that, we fitted experimental data with a dual stage model for both materials.

Moisture is suspected to diffuse first in the free volume of materials and then to bond with their bulk. With the dual stage model, stress and mass show again an excellent agreement.

Acknowledgements

This research did not receive any specific grant from funding agencies in the public, commercial, or not-for-profit sectors.

- [1] Q. Ma, Q. Tran, C. Pan, H. Fujimoto, C. Chiang, Polymer/metal interfaces in interconnect structures: Moisture diffusion and stress corrosion effects, *Mat. Res. Soc. Symp. Proc.* 511 (1998) 329-339.
- [2] M. Pecht, A model for moisture induced corrosion failures in microelectronic packages, *IEEE Trans. Components, Hybrids, Manuf. Technol.* 13 (1990) 383–389.
- [3] M.D. Groner, S.M. George, R.S. McLean, P.F. Carcia, Gas diffusion barriers on polymers using Al₂O₃ atomic layer deposition, *Appl. Phys. Lett.* 88 (2006) 1–3.
- [4] K.L. Jarvis, P.J. Evans, N.A. Cooling, B. Vaughan, J. Habsuda, W.J. Belcher, C. Bilen, G. Griffiths, P.C. Dastoor, G. Triani, Comparing three techniques to determine the water vapour transmission rates of polymers and barrier films, *Surfaces and Interfaces.* 9 (2017) 182–188.
- [5] P.F. Carcia, R.S. McLean, M.D. Groner, A.A. Dameron, S.M. George, Gas diffusion ultrabarrriers on polymer substrates using Al₂O₃ atomic layer deposition and SiN plasma-enhanced chemical vapor deposition, *J. Appl. Phys.* 106 (2009) 1–6.
- [6] R. Paetzold, A. Winnacker, D. Henseler, V. Cesari, K. Heuser, Permeation rate measurements by electrical analysis of calcium corrosion, *Rev. Sci. Instrum.* 74 (2003) 5147–5150.
- [7] R.M. Barrer, *Diffusion in and through solids*, Cambridge University Press, Cambridge, 1941.
- [8] J. Crank, *Diffusion in polymers*, Academic Press, London, 1968.
- [9] J.E. Shelby, *Handbook of gas diffusion in solids and melts*, ASM International, 1996.
- [10] R.H. Doremus, Diffusion of water in silica glass, *J. Mater. Res.* 10 (1995) 2379–2389.

- [11] K.M. Davis, M. Tomozawa, Water diffusion into silica glass - Structural-changes in silica glass and their effect on water solubility and diffusivity, *J. Non. Cryst. Solids*. 185 (1995) 203–220.
- [12] E.J. Mcinerney, P.A. Flinn, Diffusivity of moisture in thin film, 20th Int. Rel. Phy. Symp. (1982) 264–267.
- [13] C. Regard, C. Gautier, H. Fremont, P. Poirier, M.A. Xiaosong, K.M.B. Jansen, Fast reliability qualification of SiP products, *Microelectron. Reliab.* 49 (2009) 958–962.
- [14] B. Visweswaran, P. Mandlik, S.H. Mohan, J.A. Silvernail, R. Ma, J.C. Sturm, S. Wagner, Diffusion of water into permeation barrier layers, *J. Vac. Sci. Technol. A* 33 (2015) 031513.
- [15] G.G. Stoney, The tension of metallic films deposited by electrolysis, *Proc. R. Soc. Lond. A* 82 (1909) 172–175.
- [16] A. Mézin, Coating internal stress measurement through the curvature method : A geometry-based criterion delimiting the relevance of Stoney ' s formula, *Surf. Coatings Technol.* 200 (2006) 5259–5267.
- [17] J. Crank, *The Mathematics of Diffusion*, Oxford University Press, 1975.
- [18] V.P. Tolstoy, I.V. Chernyshova, V.A. Skyrshesky, *Handbook of infrared spectroscopy of ultrathin films*, John Wiley and Sons Inc, Hoboken, NJ, (2003) 243–286.
- [19] J. Thurn, Water diffusion coefficient measurements in deposited silica coatings by the substrate curvature method, *J. Non. Cryst. Solids*. 354 (2008) 5459–5465.
- [20] G. Xu, D.R. Clarke, Q. Ma, H. Fujimoto, Moisture diffusion along the TiN / SiO₂ interface and in plasma-enhanced chemical vapor deposited SiO₂, *J. Appl. Phys.* 88 (2000) 3695–3698.

- [21] Y. He, X. Fan, In-situ characterization of moisture absorption and desorption in a thin BT core substrate, Proc. - Electron. Components Technol. Conf. (2007) 1375–1383.
- [22] C.R. Moylan, M.E. Best, M. Ree, Solubility of water in polyimides: Quartz crystal microbalance measurements, J. Polym. Sci. Part B Polym. Phys. 29 (1991) 87–92.
- [23] M.D. Placette, X. Fan, J.H. Zhao, D. Edwards, Dual stage modeling of moisture absorption and desorption in epoxy mold compounds, Microelectron. Reliab. 52 (2012) 1401–1408.

List of figures

Figure 1: (a) and (b) Infrared spectra after deposition and after moisture saturation (> 800 hours) respectively for SiO₂ and N-doped SiO₂. (c) and (d) focus on the 2800 to 3800 cm⁻¹ range after deposition and after moisture saturation (> 800 hours) respectively for SiO₂ and N-doped SiO₂.

Figure 2: (a) mass uptake (b) stress variation and (c) IR area variations (corresponding to the 2800 cm⁻¹ to 3800 cm⁻¹ area) for SiO₂ layer.

Figure 3: (a) mass uptake (b) stress variation and (c) IR area variations (corresponding to the 2800 cm⁻¹ to 3800 cm⁻¹ area) for N-doped SiO₂ layer.

Figure 4: Mass variations fitted with Fick model and dual stage model respectively for SiO₂ (a) and N-doped SiO₂ (b). Stress variations fitted with Fick model and dual stage model respectively for SiO₂ (c) and N-doped SiO₂ (d).

Table captions

Table 1: Material properties after deposition.

Table 2: Diffusion coefficients of moisture and saturated moisture concentrations obtained with mass, stress and infrared spectroscopy measurements at 21°C and 40% RH.

Table 3: Diffusion coefficients of moisture for similar materials.

Table 4: Uncertainties and minimal variations to obtain diffusion parameters.

Table 5: Deviation data (S from Eq. (6)) calculated for Fick model and dual stage model for both materials.

Table 6: Diffusion parameters for SiO₂ and N-doped SiO₂ with dual stage model.

Figure 1:

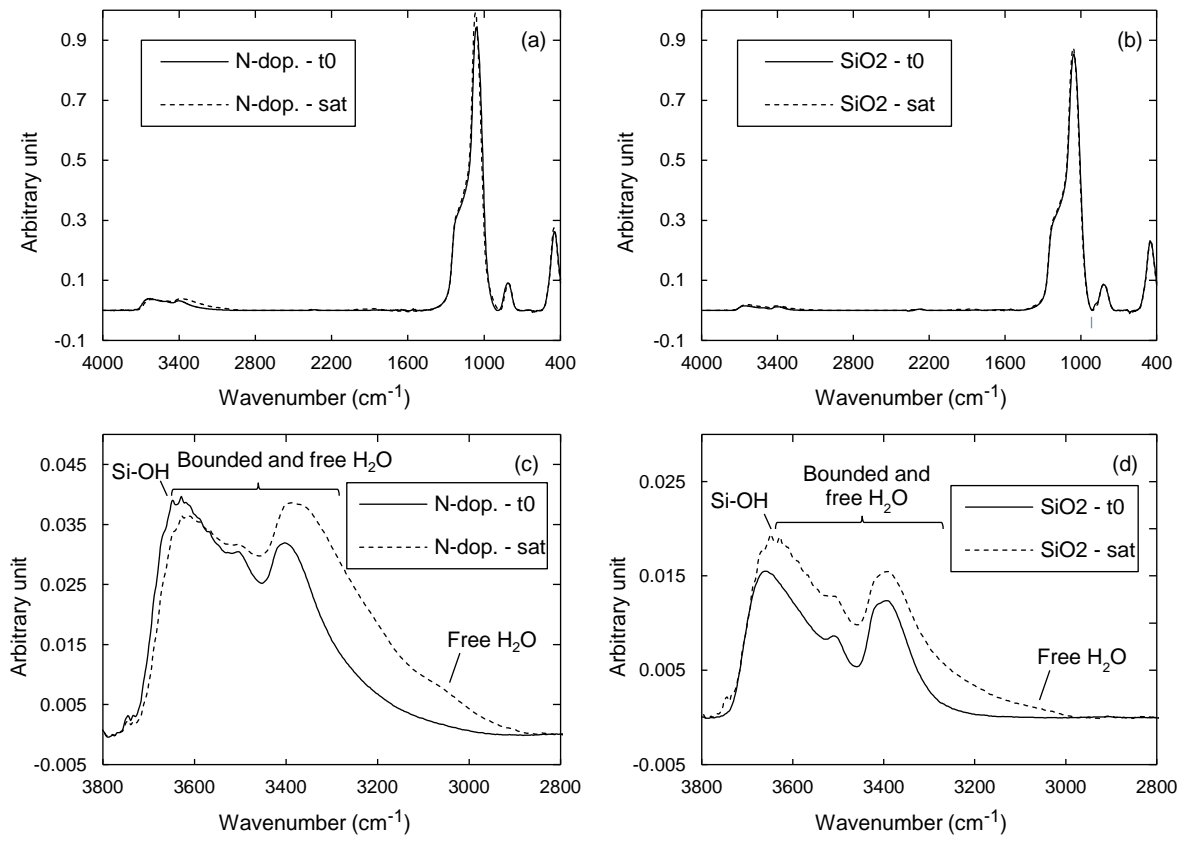


Figure 2:

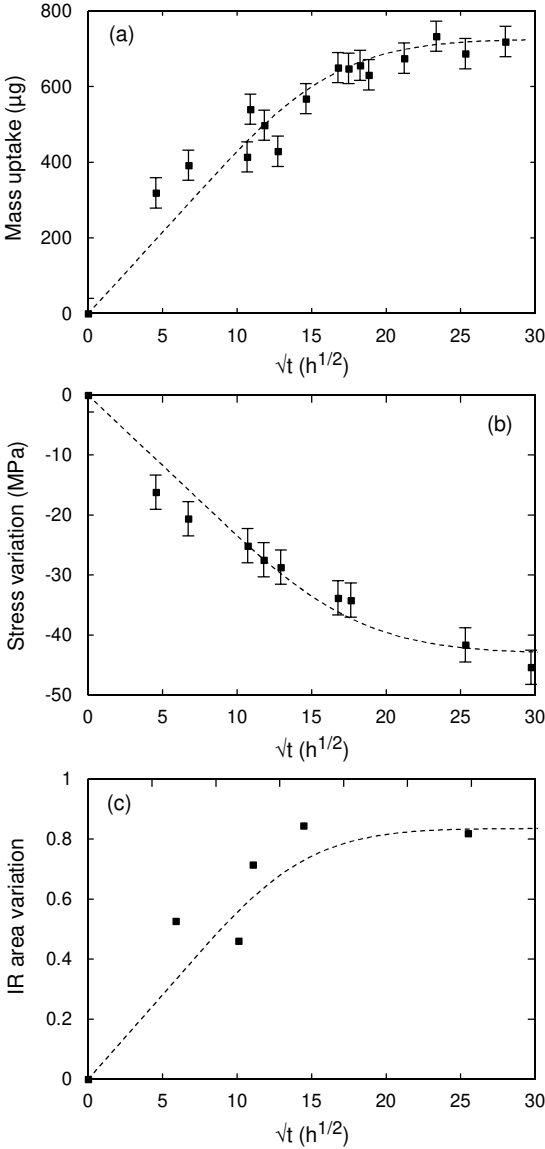


Figure 3:

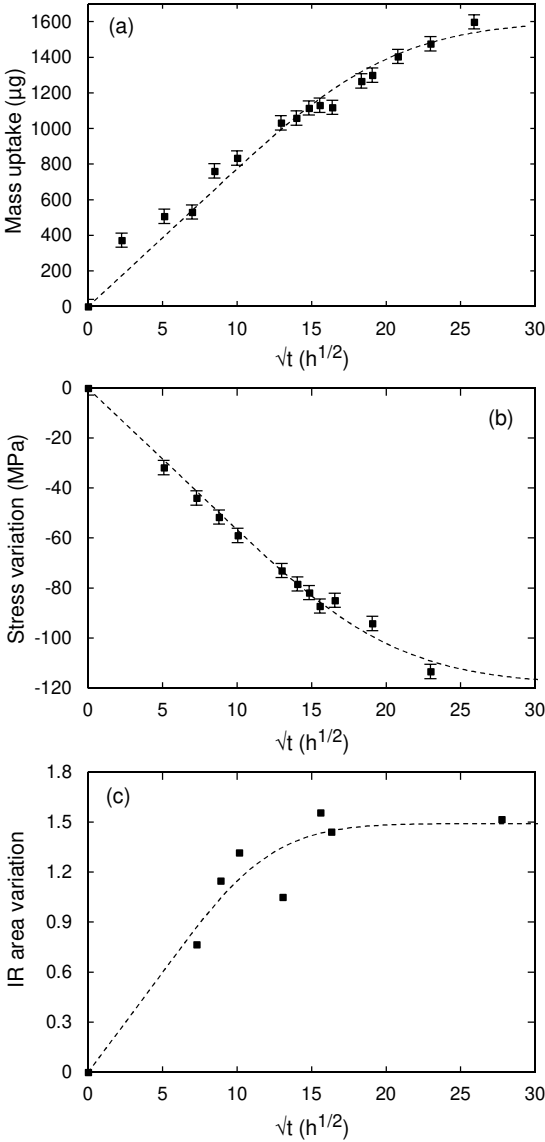


Figure 4:

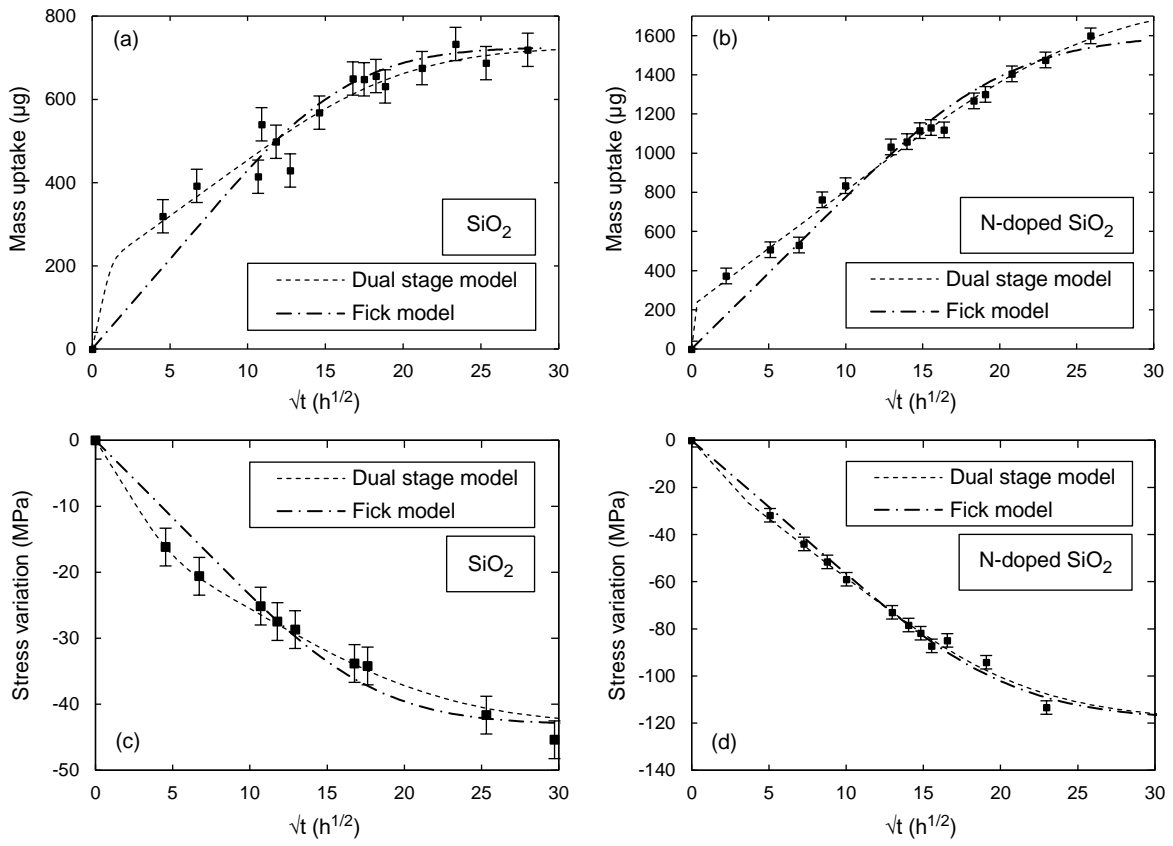


Table 1:

	Thickness (nm)	Intrinsic stress (MPa)
SiO ₂ :H	600	80
N-doped SiO ₂ :H	550	-50

Table 2:

		Mass	Stress	IR spectroscopy
SiO₂ (400°C)	D (cm².s⁻¹)	2.8×10^{-15}	2.3×10^{-15}	3.6×10^{-15}
	C_{sat} (mg.cm⁻³)	17		
N-doped SiO₂ (200°C)	D (cm².s⁻¹)	1.6×10^{-15}	1.5×10^{-15}	4.2×10^{-15}
	C_{sat} (mg.cm⁻³)	41		

Table 3:

Material	Permeant	D (cm².s⁻¹)	Env. conditions	Ref
SiO ₂ -silicone hybrid	H ₂ O	5.4×10^{-17}	38°C/90% RH	[14]
Sputtered silica	H ₂ O	1.0×10^{-13}	25°C/100% RH	[19]
PECVD Silica	D ₂ O, H ₂ ¹⁸ O	$(7 \pm 2) \times 10^{-17}$	Room T°	[20]
CVD phosphosilicate glass	H ₂ O	10^{-14}	23°C	[12]
PECVD SiO ₂ (400°C)	H ₂ O	$[2.3-2.8] \times 10^{-15}$	21°C/40% RH	This work
PECVD N-doped SiO ₂ (200°C)	H ₂ O	$[1.5-1.6] \times 10^{-15}$	21°C/40% RH	This work

Table 4:

	Mass	Bending radius of curvature	IR
Uncertainty	40 μg	0.5 μm	/
Minimal variation	> 0.25% in mass	$\Delta R = 5 \mu\text{m}$ $\Delta\sigma = 13 \text{ MPa}$ > 0.25% in mass	> 0.8% in mass

Table 5:

		N-doped SiO₂		SiO₂	
		Mass	Stress	Mass	Stress
S	Fick model	89 833 μg^2	326 MPa^2	47 968 μg^2	83 MPa^2
	Dual stage model	30 793 μg^2	318 MPa^2	22 203 μg^2	26 MPa^2

Table 6:

		N-doped SiO ₂		SiO ₂	
		Mass	Stress	Mass	Stress
Dual stage model	D ₁ (cm ² .s ⁻¹)	2.2 × 10 ⁻¹²	1.9 × 10 ⁻¹²	5.7 × 10 ⁻¹³	3.1 × 10 ⁻¹⁴
	D ₂ (cm ² .s ⁻¹)	1.5 × 10 ⁻¹⁵	1.4 × 10 ⁻¹⁵	2.0 × 10 ⁻¹⁵	1.5 × 10 ⁻¹⁵
	X _{1,∞}	219 μg (14% of total uptake)	-8 MPa (7% of total variation)	185 μg (26% of total uptake)	-12 MPa (28% of total variation)
	X _{2,∞}	1380 μg	-110 MPa	540 μg	-31 MPa